Resonance Raman Investigation of the Au(I)−Au(I) Interaction of the $^1[d\sigma^*p\sigma]$ Excited State of $Au_2(dcpm)_2(ClO_4)_2$ (dcpm = Bis(dicyclohexylphosphine)methane)

King Hung Leung, David Lee Phillips,* Man-Chung Tse, Chi-Ming Che,* and Vincent M. Miskowski

Contribution from the Department of Chemistry, The University of Hong Kong, Pokfulam Road, Hong Kong

Received January 20, 1999

Abstract: We present a resonance Raman investigation of the lowest energy dipole-allowed absorption band of $[Au_2(dcpm)_2](ClO_4)_2$ (dcpm = bis(dicyclohexylphosphine)methane). The resonance Raman spectra provide the first experimental proof of the $5d\sigma^* \rightarrow 6p\sigma$ electronic transition in dinuclear gold(I)−phosphine compounds. A resonance Raman intensity analysis of the spectra allows estimation of the structural changes of the $[d\sigma^*p\sigma]$ excited states relative to the ground state.

Introduction

Luminescent gold(I) compounds, and in particular those with intramolecular gold−gold interactions, have been receiving intense interest from different perspectives.[1−8] Extensive photoluminescence measurements have been made on this class of compounds, and in many instances the relationship between aurophilicity (i.e., gold−gold bonding) and the emission energies has been stated.[1] It has also been reported that dinuclear and polynuclear gold(I) compounds with bridging phosphine ligands have long-lived emissive excited states which are powerful photoreductants with $E°$ values ranging from −1.6 to −1.7 V vs SCE[5f,6a] Indeed, interesting photochemistry has been reported for the $[Au_2(dppm)_2]^{2+}$ (dppm = bis(diphenylphosphine)-methane) complex which catalyzes reductive C−C bond coupling from alkyl halides upon photoexcitation with UV light and in the presence of sacrificial electron donors.[5b]

Like d^8−d^8 metal complexes,[9] metal−metal interaction in dinuclear gold(I) compounds leads to an intense low-energy $nd\sigma^* \rightarrow (n+1)p\sigma$ transition, which red-shifts in energy from the $nd\sigma^* \rightarrow (n+1)p\sigma$ transition of its mononuclear counterparts.[4,5a,10] Here, the $nd\sigma^*$ refers to the antibonding combination of nd_{z^2} and $(n+1)p\sigma$ to the bonding combination of the $(n+1)p_z$ orbitals. The prototype example of dinuclear gold(I) compounds is $[Au_2(dppm)_2]^{2+}$, which exhibits an intense $5d\sigma^* \rightarrow 6p\sigma$ transition at 297 nm.[4,5a] In solution, this compound shows a long-lived photoluminescence at 570 nm, which was assigned to come from the $^3[d\sigma^*p\sigma]$ excited state. Recent molecular orbital studies revealed that such an assignment needs to be revised.[11] The $^3[d\sigma^*p\sigma]$ excited state of $[Au_2(H_2PCH_2PH_2)_2]^{2+}$ was calculated to have a gold−gold single bond and readily forms a metal−metal-bonded solvent/anion exciplex in solution at room temperature.[11,12] Clearly, the excited states associated with the $5d\sigma^* \rightarrow 6p\sigma$ transition have interesting photophysical and photochemical properties, but because of the lack of vibronic structure in this absorption band, the structural change of the excited state(s) relative to the ground state can only be inferred from the molecular orbital calculations. Here, we report a resonance Raman investigation of the lowest energy dipole-allowed absorption band of $[Au_2(dcpm)_2](ClO_4)_2$ (dcpm = bis-(dicyclohexylphosphine)methane), which provides the first experimental proof of the $5d\sigma^* \rightarrow 6p\sigma$ electronic transition in dinuclear gold(I)−phosphine compounds and provides information that allows estimation of structural changes of the $[d\sigma^*p\sigma]$ excited states relative to the ground state. The choice of the dcpm ligand is because its intraligand transitions occur at energies much higher than that of the $5d\sigma^* \rightarrow 6p\sigma$ transition.

Experiment

The preparation and crystal structure of $[Au_2(dcpm)_2](ClO_4)_2$ will be described elswhere.[12] The resonance Raman experiments used sample solutions with concentrations in the 5−10 mM range for $[Au_2(dcpm)_2]$-

* To whom correspondence should be addressed.

(1) Gade, L. H. *Angew. Chem., Int. Ed. Engl.* **1997**, *36*, 1171−1173.
(2) Vickery, J. C.; Olmstead, M. M.; Fung, E. Y.; Balch, A. L. *Angew. Chem., Int. Ed. Engl.* **1997**, *36*, 1179−1181.
(3) Mansour, M. A.; Connick, W. B.; Lachicotte, R. J.; Gysling, H. J.; Eisenberg, R. *J. Am. Chem. Soc.* **1998**, *120*, 1329−1330.
(4) King, C.; Wang, J.-C.; Khan, Md. N. I.; Fackler, J. P. *Inorg. Chem.* **1989**, *28*, 2145−2149.
(5) (a) Che, C.-M.; Kwong, H.-L.; Yam, V. W. W.; Cho, K. C. *J. Chem. Soc., Chem. Commun.* **1989**, 885−886. (b) Li, D.; Che, C.-M., Kwong, H. L.; Yam, V. W. W. *J. Chem. Soc., Dalton Trans.* **1992**, 3325−3329. (c) Shieh, S. J.; Hong, X.; Peng, S. M.; Che, C.-M. *J. Chem. Soc., Dalton Trans.* **1994**, 3067−3068. (d) Tzeng, B. C.; Cheung, K. K.; Che, C.-M. *Chem. Commun.* **1996**, 1681−1682. (e) Tzeng, B. C.; Chan, C. K.; Cheung, K. K.; Che, C. M.; Peng, S. M. *Chem. Commun.* **1997**, 135−136. (f) Weng, Y.-X.; Chan, K. C.; Tzeng, B. C.; Che, C. M. *J. Chem. Phys.* **1998**, 109, 5948−5956.
(6) (a) Yam, V. W. W.; Lai, T. F.; Che, C.-M. *J. Chem. Soc., Dalton Trans.* **1990**, 3747−3752. (b) Yam, V. W. W.; Li, C. K.; Chan, C. L. *Angew. Chem., Int. Ed. Engl.* **1998**, *37*, 2857−2859.
(7) Bowmaker, G. A. In *Gold, Progress in Chemistry, Biochemistry and Technology*; Schmidbaur, H., Ed.; Wiley: New York, 1999.
(8) Forward, J. M.; Fackler, J. P.; Assefa, Z. In *Optoelectronic Properties of Inorganic Compounds*; Roundhill, D. M., Fackler, J. P., Eds.; Plenum: New York, 1999; pp 195−230.
(9) (a) Lewis, N. S.; Mann, K. R.; Gordon, J. G., II; Gray, H. B. *J. Am. Chem. Soc.* **1976**, *98*, 7461−7463. (b) Rice, S. F.; Gray, H. B. *J. Am. Chem. Soc.* **1981**, *103*, 1593−1595. (c) Roundhill, D. M.; Gray, H. B.; Che, C. M. *Acc. Chem. Res.* **1989**, *22*, 55−61.
(10) Jaw, H.-R. C.; Savas, M. M.; Rogers, R. D.; Mason, W. R. *Inorg. Chem.* **1989**, *28*, 1028−1037.
(11) Zhang, H. Z.; Che, C. M. *Chem. Eur. J.*, in press.
(12) Fu, W. F.; Chan, K. C.; Cheung, K. K., Miskowski, V. M.; Che, C. M. *Angew. Chem., Int. Ed. Engl.*, submitted for publication.

10.1021/ja990195e CCC: $18.00
Published on Web 05/11/1999

$(ClO_4)_2$ in spectroscopic grade acetonitrile solvent. The resonance Raman apparatus and methods have been previously described,[13] so only a brief description is given here. The excitation frequencies were obtained from the harmonics and hydrogen Raman shifted laser lines from a Nd:YAG. A loosely focused laser beam (~1 mm diameter) excited the samples held in a stirred UV-grade quartz cell. An ~130° back-scattering geometry was used to collect the Raman signal with reflective optics and image the light through a depolarizer and the entrance slit of a 0.5 m spectrograph. The light was dispersed onto a liquid nitrogen cooled CCD detector by a 1200 groove/mm ruled grating blazed at 250 nm. About 30−60 1−2 min scans collected from the CCD were added together to find the resonance Raman spectrum.

Known acetonitrile solvent bands and Hg lamp emission lines were used to calibrate the Raman shifts of the resonance Raman spectra. The resonance Raman spectra were intensity corrected for any remaining sample reabsorption and the wavelength dependence of the detection system response. Appropriately scaled solvent and quartz cell background spectra were subtracted to remove the solvent bands, the Rayleigh line, and the quartz cell background signal. Portions of the spectra were fit to a baseline plus a sum of Lorentzian bands to obtain the integrated areas of the Raman bands.

Previously determined absolute Raman cross sections of acetonitrile solvent bands were used as a reference[14] to measure the absolute resonance Raman cross sections of $[Au_2(dcpm)_2](ClO_4)_2$. A UV/vis spectrometer was used to measure the concentrations of the sample solutions, and changes of less than 5% were observed for the absorption spectra for the absolute Raman cross section measurements. The absolute resonance Raman cross sections were calculated from the average of a series of measurements. The depolarization ratio of the ν_{Au-Au} band of $[Au_2(dcpm)_2](ClO_4)_2$ and its first overtone in the 282.4 nm resonance Raman spectrum was determined to be ~0.35, and this value was used to calculate the absolute Raman cross section. The absolute resonance Raman cross sections displayed little power dependence over a range of 0.1−1.5 mW with differences of less than 5%. The maximum molar extinction coefficient was determined to be 25 400 M^{-1} cm^{-1} for the ~277 nm absorption band of $Au_2(dcpm)_2(ClO_4)_2$ in acetonitrile solution.

Calculations

The simulations given here are meant to determine a reasonable estimate of the structural changes associated with the ~277 nm absorption band of $Au_2(dcpm)_2(ClO_4)_2$. These results will also provide a useful reference to which more sophisticated simulations can be compared to assess the relative importance of effects such as changes in the transition dipole moment with vibrational coordinate and anharmonicity on the resonance Raman and absorption spectra. The resonance Raman intensities and absorption spectra were calculated using a time-dependent formalism.[15−22] The absorption cross sections were computed from

$$\sigma_A(E_L) = (4\pi e^2 E_L M^2/3n\hbar^2 c)\int_{-\infty}^{\infty} d\delta\ G(\delta) \sum_i P_i Re[\int_0^{\infty} \langle i|i(t)\rangle \times \exp[i(E_L + \epsilon_i)t/\hbar] \exp[-g(t)]\, dt] \quad (1)$$

and the resonance Raman cross sections were calculated from

$$\sigma_R(E_L,\omega_s) = \int_{-\infty}^{\infty} d\delta\ G(\delta) \sum_i \sum_f P_i \sigma_{R,i\rightarrow f}(E_L)\ \delta(E_L+\epsilon_i-E_S-\epsilon_f)$$

with

$$\sigma_{R,i\rightarrow f}(E_L) = (8\pi e^4 E_S 3E_L M^4/9\hbar^6 c^4)|\int_0^{\infty} \langle f|i(t)\rangle \exp[i(E_L + \epsilon_i)t/\hbar] \exp[-g(t)]\, dt|^2 \quad (2)$$

where n is the solvent index of refraction, M is the transition length evaluated at the equilibrium geometry, E_L is the incident photon energy, E_S is the scattered photon energy, f is the final state for the resonance Raman process, ϵ_f is the energy of the ground-state energy level $|f\rangle$, and $\delta(E_L+\epsilon_i-E_S-\epsilon_f)$ is a delta function to sum up cross sections with the same frequency. P_i is the initial Boltzmann population of the ground-state energy level $|i\rangle$ which has energy ϵ_i. $|i(t)\rangle = e^{-iHt/\hbar}|i\rangle$ is $|i(t)\rangle$ propagated on the excited-state surface for a time t and H is the excited-state vibrational Hamiltonian. The absorption and resonance Raman cross sections were computed using an addition over a ground-state 298 K Boltzmann distribution of vibrational energy levels. The Condon approximation was used, and the ground- and excited-state potential energy surfaces were approximated by harmonic oscillators displaced by Δ in dimensionless normal coordinates. The time-dependent overlaps in eqs 1 and 2 were computed numerically from analytic formulations of Mukamel and co-workers.[23]

We carried out calculations with the damping function $\exp[-g(t)]$ term in eqs 1 and 2 modeled as a simple exponential decay function (where the $\exp[-g(t)]$ term in eqs 1 and 2 was replaced by $\exp[-t/\tau]$ with τ the dephasing time) or as a Brownian oscillator. For the Brownian oscillator dephasing function simulations, the $g(t)$ function has the following form in eqs 1 and 2:

$$g(t) = (D/\Lambda)^2(\Lambda t - 1 + \exp(-\Lambda t)) + i(D^2\Lambda/2kT)(1 - \exp(-\Lambda t)) + t/\tau \quad (3)$$

where the solvent random perturbations cause the solute energy levels to fluctuate with D magnitude and Λ frequency.[24] We assumed that that the temperature (T) is large enough that the solvent mode frequencies are $\ll kT$[24] and that all the solvent modes were grouped together into one effective mode. The t/τ term in eq 3 is the pure lifetime decay.

Results and Discussion

The use of resonance Raman spectroscopy to study the ligand to metal charge transfer excited states of gold(I) thiolates has been previously reported by Zink and co-workers.[25] Figure 1 shows the geometry and absorption spectrum of $[Au_2(dcpm)_2](ClO_4)_2$ (**1**) in acetonitrile solution with the excitation wavelengths for the resonance Raman experiments displayed above the absorption spectrum. Figure 2 shows an unprocessed resonance Raman spectrum obtained with 282.4 nm excitation and the same resonance Raman spectrum after intensity corrections and subtractions of the Rayleigh line, glass bands, and solvent bands. Figure 3 gives an overview of the resonance Raman spectra of **1** in acetonitrile solution. The resonance Raman spectra depicted in Figure 3 have almost all of their intensity in the Au−Au stretch fundamentals and overtones, and this is consistent with the proposed assignment of the absorption band at ~277 nm to be due to $d\sigma^* \rightarrow p\sigma$ transitions.[4,5a,11] The

(13) (a) Kwok, W. M.; Phillips, D. L.; Yeung, P. K.-Y.; Yam, V. W. W. *Chem. Phys. Lett.* **1996**, *262*, 699−708. (b) Kwok, W. M.; Phillips, D. L.; Yeung, P. K.-Y.; Yam, V. W. W. *J. Phys Chem. A* **1997**, *101*, 9286−9295. (c) Zheng, X.; Phillips, D. L. *J. Chem. Phys.* **1998**, 5772−5783.

(14) (a) Trulson, M. O.; Mathies, R. A. *J. Chem. Phys.* **1986**, *84*, 2068−2074. (b) Dudik, J. M.; Johnson, C. R.; Asher, S. A. *J. Chem. Phys.* **1985**, *82*, 1732−1740.

(15) Lee, S. Y.; Heller, E. J. *J. Chem. Phys.* **1979**, *71*, 4777−4788.

(16) Myers, A. B.; Mathies, R. A.; Tannor, D. J.; Heller, E. J. *J. Chem. Phys.* **1982**, *77*, 3857−3866.

(17) Tutt, L.; Tannor, D.; Heller, E. J.; Zink, J. I. *Inorg. Chem.* **1982**, *21*, 3858−3859.

(18) Myers, A. B.; Mathies, R. A. *Biological Applications of Raman Spectroscopy*; Wiley: New York, 1987; pp 1−58.

(19) Clark, R. J. H.; Dines, T. J. *Angew. Chem., Int. Ed. Engl.* **1986**, *98*, 131−160.

(20) (a) Doorn, S. K.; Hupp, J. T. *J. Am. Chem. Soc.* **1989**, *111*, 1142−1144. (b) Doorn, S. K.; Hupp, J. T.; Porterfield, D. R.; Campion, A.; Chase, D. B. *J. Am. Chem. Soc.* **1990**, *112*, 4999−5002. (c) Blackbourn, R. L.; Johnson, C. S.; Hupp, J. T.; Bryant, M. A.; Sobocinski, R. L.; Pemberton, J. E. *J. Phys. Chem.* **1991**, *95*, 10535−10537.

(21) Zink, J. I.; Shin, K. S. K. *Adv. Photochem.* **1991**, *16*, 119−214.

(22) Myers, A. B. *Laser Techniques in Chemistry*; Wiley: New York, 1995; pp 325−384.

(23) Yan, Y. J.; Mukamel, S. *J. Chem. Phys.* **1987**, *86*, 6085−6107.

(24) Li, B.; Johnson, A. E.; Mukamel, S.; Myers, A. B. *J. Am. Chem. Soc.* **1994**, *116*, 11039−11047.

(25) Hanna, S. D.; Khan, S. I.; Zink, J. I. *Inorg. Chem.* **1996**, *35*, 5813−5819.

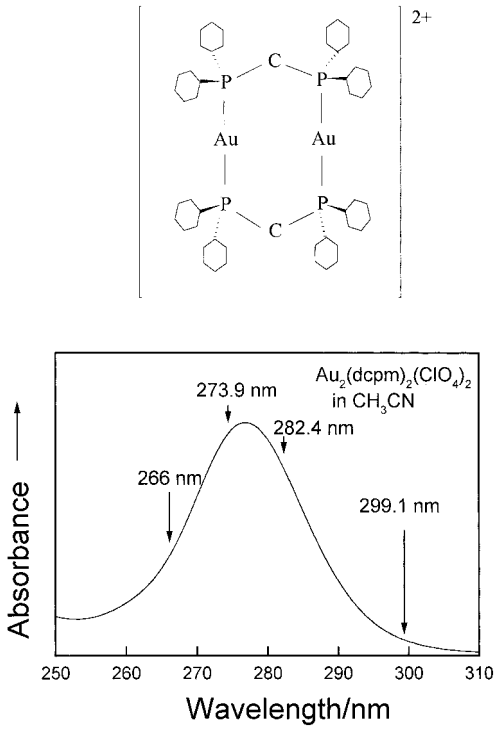

Figure 1. (Top) Geometry of $Au_2(dcpm)_2(ClO_4)_2$ (**1**). (Bottom) Absorption spectra of $Au_2(dcpm)_2(ClO_4)_2$ (**1**) in acetonitrile solution at room temperature with the excitation wavelengths for the resonance Raman experiments indicated above the spectrum.

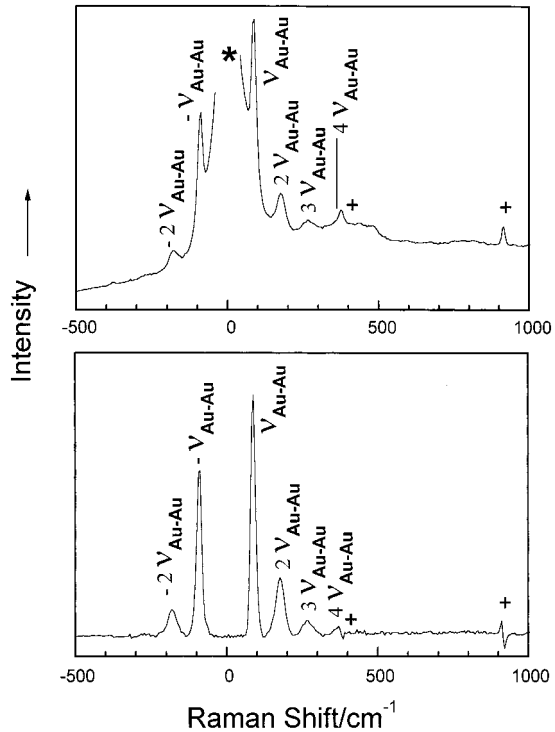

Figure 2. (Top) Raw resonance Raman spectrum of $Au_2(dcpm)_2(ClO_4)_2$ (**1**) in acetonitrile solution at room temperature taken with 282.4 nm excitation. (Bottom) The same resonance Raman spectrum in (A) after intensity corrections and subtractions of the Rayleigh line, glass bands, and solvent bands.

fundamental frequency for the resonance Raman spectra of **1** is 88 cm^{-1} in good agreement with the Au−Au stretch peak found in nonresonant Raman spectra.[26,27] Table 1 lists the Raman

(26) Tse, M. C. Ph.D. Thesis, The University of Hong Kong, 1999.

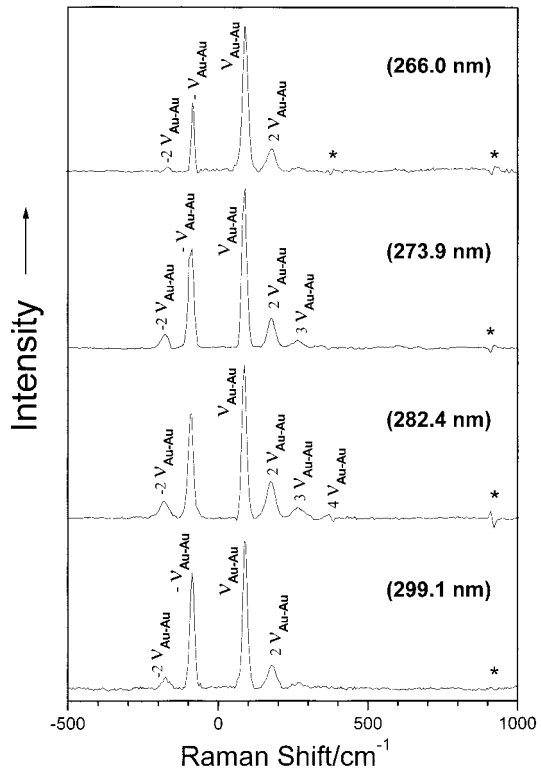

Figure 3. Overview of the resonance Raman spectra of $Au_2(dcpm)_2(ClO_4)_2$ (**1**) in acetonitrile solution obtained with 266.0, 273.9, 282.4, and 299.1 nm excitation wavelengths. The spectra have been intensity corrected, and the Rayleigh line, glass bands, and solvent bands have been subtracted. Asterisks mark regions were solvent subtraction artifacts are present. The assignments of the more intense Raman bands are shown next to the bands.

shifts, relative resonance Raman intensities, and absolute resonance Raman cross section values found from the experimental resonance Raman spectra shown in Figure 3.

We have simultaneously simulated the absorption spectra and resonance Raman intensities of **1** using time-dependent wave packet calculations so as to estimate the structural change of the excited electronic state relative to the ground electronic state. Our first set of calculations used a simple exponential decay function to model the spectral broadening due to solvent dephasing, and our second set of calculations used an overdamped Brownian oscillator function to simulate the solvent dephasing. The simple exponential decay function for the spectral broadening due to solvent dephasing is not very realistic since it considers only the effect of the solvent on the solute electronic transition and not vice versa. An overdamped Brownian oscillator function for the solvent dephasing provides a somewhat more realistic model in that it can account for solvent reorganization and the Stokes shift between absorption and emission.[24] We used a simple overdamped Brownian oscillator with a single effective mode given by eq 3 in the Calculations. The best fit modeling parameters for both sets of simulations are shown in Table 2 for **1**. Figures 4 and 5 compare the computed and experimental absorption spectra and resonance Raman intensities for **1**. There is reasonable agreement between the experimental and calculated absorption spectra and resonance Raman intensities for both sets of calculations as shown in Figures 4 and 5. There is also good agreement between the calculated and experimental absolute resonance Raman cross sections listed in Table 1.

(27) Perreault, D.; Drouin, M.; Michel, A.; Miskowski, V. M.; Schaefer, W. P.; Harvey, P. D. *Inorg. Chem.* **1992**, *31*, 695−702.

Table 1. Resonance Raman Bands of $Au_2(dcpm)_2(ClO_4)_2$ **1** in Acetonitrile Solution

Raman band	Raman shift[a] (cm^{-1})	intensity[b] 266.0 nm	273.9 nm	282.4 nm	299.1 nm
$-2\nu_{Au-Au}$	−176	9	19	20	20
$-\nu_{Au-Au}$	−88	80	104	164	202
ν_{Au-Au}	88	199	254	309	288
$2\nu_{Au-Au}$	176	100	100	100	100
absolute Raman cross section of $2\nu_{Au-Au}$ ($Å^2$/molecule)					
exptl		1.4×10^{-8}	2.4×10^{-8}	1.1×10^{-8}	2.6×10^{-10}
calcd[c]		1.6×10^{-8}	2.8×10^{-8}	1.0×10^{-8}	2.9×10^{-10}
calcd[d]		1.4×10^{-8}	2.0×10^{-8}	1.0×10^{-8}	3.6×10^{-10}
$3\nu_{Au-Au}$	265	25	27	22	12
$4\nu_{Au-Au}$	350			4	

[a] Estimated uncertainties are about 4 cm^{-1} for the Raman shifts. [b] Relative intensities are based on integrated areas of Raman bands. Estimated uncertainties are about 5% for intensities greater than 100, 10% for intensities between 50 and 100, and 20% for intensities below 50. [c] Calculated using the parameters of Table 2A in eqs 1 and 2 and the exponential decay damping function for solvent dephasing. [d] Calculated using the parameters of Table 2B in eqs 1 and 2 and the overdamped Brownian oscillator damping function for solvent dephasing.

Table 2. Parameters for Simulations of Resonance Raman Intensities and Absorption Spectra of $Au_2(dcpm)_2(ClO_4)_2$ (**1**) in Acetonitrile Solution

A. Parameters for Simulations Using the Exponential Decay Damping Function

ground-state vibrational frequency (cm^{-1})	excited-state vibrational frequency (cm^{-1})	Δ
88	175	0.68

$E_0 = 35\,950$ cm^{-1}, $M = 1.11$ Å, $n = 1.344$
homogeneous broadening, $\Gamma = 1600$ cm^{-1} fwhm
inhomogeneous broadening, $G = 500$ cm^{-1} std dev

B. Parameters for Simulations Using the Overdamped Brownian Oscillator Damping Function

ground-state vibrational frequency (cm^{-1})	excited-state vibrational frequency (cm^{-1})	Δ
88	175	0.68

$E_0 = 34\,000$ cm^{-1}, $M = 0.995$ Å, $n = 1.344$
homogeneous broadening, $\Gamma = 2150$ cm^{-1} fwhm
inhomogeneous broadening, $G = 200$ cm^{-1} std dev
Brownian oscillator $\Lambda/D = 0.06$, $\Lambda = 55.3$ cm^{-1}, $D = 2048$ cm^{-1}

The best fit parameters for the first set and second set of calculations give similar agreement between the computed and experimental absorption spectra and resonance Raman intensities (see Figures 4 and 5 and Table 1). The ground- and excited-state frequencies as well as the normal mode displacement parameters do not noticeably change when using the two different damping functions. However, there are some minor changes in the other simulation parameters when the two different solvent dephasing damping functions are used. The zero−zero energy, E_0, for the excited electronic state becomes lower by approximately the solvent reorganizational energy when using the overdamped Brownian oscillator solvent dephasing function (e.g., $E_0 = 35\,950$ cm^{-1} for **1** with the exponential decay damping and $E_0 = 34\,000$ cm^{-1} for overdamped Brownian oscillator damping with $D = 2048$ cm^{-1}). When the solvent dephasing contribution to the absorption bandwidth is fairly large (such as ∼2000 cm^{-1} for the ∼277 nm absorption of **1**), the simulations using the somewhat more realistic overdamped Brownian oscillator damping function should provide a noticeably better estimate of E_0 than a simple exponential decay damping function. The differing damping functions also give rise to minor differences in the transition lengths (exponential decay damping gives $M = 1.11$ Å for **1** compared to $M = 0.995$ Å for **1** using the overdamped Brownian oscillator function) and also the homogeneous broadening parameters (exponential decay damping gives $\Gamma = 1600$ cm^{-1} for **1** compared to $\Gamma = 2150$ cm^{-1} for **1** using the overdamped Brownian oscillator function). This is mostly due to the different line shapes that arise from using the two different solvent dephasing functions (see calculated absorption spectra in Figures 4 and 5).

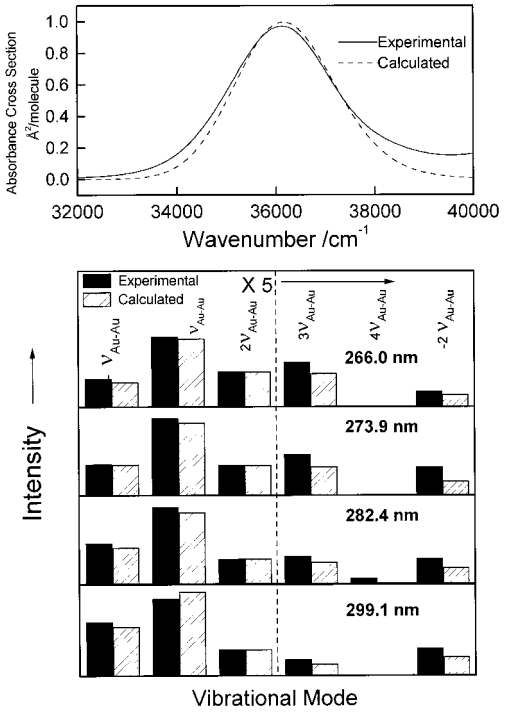

Figure 4. (Top) Comparison of the calculated (dashed line) and experimental (solid line) absorption spectra for $Au_2(dcpm)_2(ClO_4)_2$ (**1**) in acetonitrile solution. (Bottom) Comparison of the calculated (dashed bar) and experimental (solid bar) resonance Raman intensities for 266.0, 273.9, 282.4, and 299.1 nm excitation. The parameters given in Table 2A for $Au_2(dcpm)_2(ClO_4)_2$ (**1**) were used in eqs 1 and 2 to calculate the absorption and resonance Raman intensities (the model described in the Calculations and an exponential decay solvent dephasing function were used for these calculations).

We can use the normal mode displacements shown in Table 2 to estimate the change of the Au−Au bond length in the excited electronic state relative to the ground electronic state. If we assume that the Au−Au vibration is approximately a pure metal−metal stretch, then we can estimate the change in the bond length using the following equation:[22]

$$q = (\mu\omega/\hbar)^{1/2}(\Delta x) \qquad (4)$$

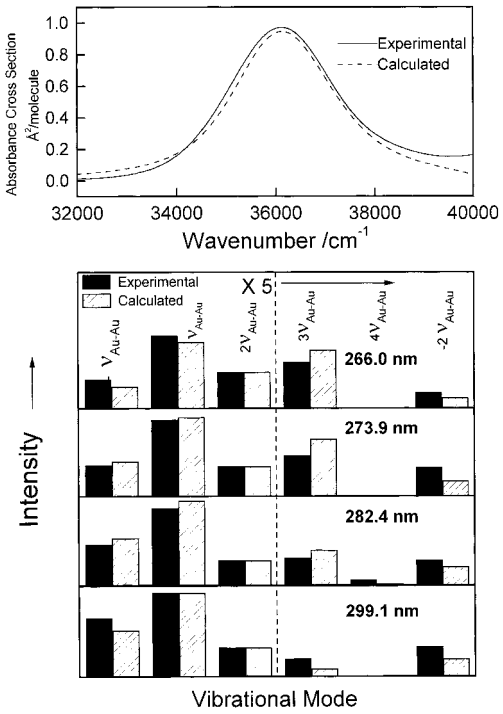

Figure 5. (Top) Comparison of the calculated (dashed line) and experimental (solid line) absorption spectra for $Au_2(dcpm)_2(ClO_4)_2$ (**1**) in acetonitrile solution. (Bottom) Comparison of the calculated (dashed bar) and experimental (solid bar) resonance Raman intensities for 266.0, 273.9, 282.4, and 299.1 nm resonance Raman spectra. The parameters given in Table 2B for $Au_2(dcpm)_2(ClO_4)_2$ (**1**) were used in eqs 1 and 2 to calculate the absorption and resonance Raman intensities (the model described in the Calculations and an overdamped Brownian oscillator solvent dephasing function were used for these calculations).

where q is the dimensionless normal coordinate, μ is the reduced mass of the metal−metal bond, ω is the ground-state vibrational frequency, and Δx is the change in the bond length. The Au−Au bond length changes by about 0.11 Å for **1** in the initially $^1[d\sigma^*p\sigma]$ excited state relative to the ground state. Thus, the Au−Au distance in the $^1[d\sigma^*p\sigma]$ excited state is ∼2.81 Å, which is not much longer than the Au(II)−Au(II) single bond distances of 2.674(1) Å in $[Au(CH_2)_2PPh_2]_2(CH_3)Br$[28] and 2.6112(7) Å in $[Au(dppn)Cl]_2(PF_6)_2$ (dppn = 1,8-bis(diphenylphosphinol-naphthalene).[29]

The simulation parameters given in Table 2 for **1** show a large increase in the Au−Au stretch vibrational frequency in the excited state (∼175 cm^{-1}) compared to its ground electronic state (88 cm^{-1}). Indeed, the excited-state Au−Au stretching frequency is comparable to the related (Pt−Pt) stretching frequency of 156 cm^{-1} in the $^3[d\sigma^*p\sigma]$ excited state of $[Pt_2(P_2O_5H_2)_4]^{4-}$ that is regarded to have a single metal−metal bond.[30] This is consistent with the proposed $d\sigma^* \rightarrow p\sigma$ absorption band assignment in that the $^1[d\sigma^*p\sigma]$ excited state is envisaged to have a formal metal−metal bond order of 1.[30,31] Some inhomogeneous broadening is needed to adequately simultaneously fit the absolute Raman cross sections and the absorption bandwidth for compound **1**. A probable source for this inhomogeneous broadening in compound **1** is likely to be due to formation of a metal−metal-bonded solvent and/or anion exciplex with slightly different electronic transition energies for the ^1A_u state. The X-ray crystal structure of $[Au_2(dcpm)_2](ClO_4)_2$ reveals weak cation−anion interaction in the ground state.[12] The Au atom adopts a T-shaped geometry, and the Au···O(ClO_4) distances average 3.36(2) Å.[12] Recent ab initio calculations[11] indicate that the model compound $[Au_2(H_2PCH_2PH_2)_2]^{2+}$ (**1**) does indeed interact with an acetonitrile solvent molecule weakly in the ground state but strongly in the excited state. The calculations found that structures of the uncomplexed $Au_2(H_2PCH_2PH_2)_2^{2+}$ and the $\{Au_2(H_2PCH_2PH_2)_2\cdot(MeCN)_2\}^{2+}$ complex have very similar Au−Au distances in the $^1A_{1g}$ ground electronic state (3.167 and 3.155 Å, respectively).[11] It was also found that the ^3A_u state of $\{Au_2(H_2PCH_2PH_2)_2\cdot(MeCN)_2\}^{2+}$ gives rise to a much shorter Au−Au distance (∼2.719 Å).[9] Our present resonance Raman intensity analysis of the $^1A_g \rightarrow {}^1A_u$ transition of **1** in acetonitrile solvent indicates that the ^1A_u state undergoes a moderate Au−Au bond length change consistent with a $^1A_g \rightarrow {}^1A_u$ transition of mainly p_σ-bonding character of the two Au atoms, and the significant inhomogeneous broadening needed to simultaneously model the absolute Raman cross sections and absorption bandwidth provides indirect evidence for the uncomplexed and solvent-complexed forms of **1** in acetonitrile solution.

Acknowledgment. This work was supported by grants from the Committee on Research and Conference Grants (CRCG), the Research Grants Council (RGC) of Hong Kong, the Hung Hing Ying Physical Sciences Research Fund, and the Large Items of Equipment Allocation 1993-94 from the University of Hong Kong. We acknowledge Professor A. B. Myers for providing a copy of the FORTRAN code used to carry out the time-dependent wave packet calculations of the absolute resonance Raman intensities and absorption spectrum.

JA990195E

(28) Basil, J. D.; Murray, H. H.; Fackler, J. P. Jr.; Tocher, J.; Mazany, A. M.; Trzcinska-Bancroft, B.; Knachel, H.; Dudis, D.; Delord, T.-J.; Marler, D. O. *J. Am. Chem. Soc.* **1985**, *107*, 6908−6915.

(29) Yam, V. W. W.; Choi, S. W. K.; Cheung, K. K. *Chem. Commun.* **1996**, 1173−1174.

(30) Che, C.-M.; Butler, L. G.; Gray, H. B.; Crooks, R. M.; Woodruff, W. H. *J. Am. Chem. Soc.* **1983**, *105*, 5492−5494.

(31) Dallinger, R. F.; Miskowski, V. M.; Gray, H. B.; Woodruff, W. H. *J. Am. Chem. Soc.* **1981**, *103*, 1595−1596.